



Published in final edited form as:

*Mol Cancer Res.* 2021 April ; 19(4): 573–584. doi:10.1158/1541-7786.MCR-20-0623.

## AKT1 E17K inhibits cancer cell migration by abrogating $\beta$ -catenin signaling

Sizhi Paul Gao<sup>\*,1</sup>, Amber J. Kiliti<sup>\*,1</sup>, Kai Zhang<sup>\*,1</sup>, Naresh Vasani<sup>1</sup>, Ninghui Mao<sup>1</sup>, Emmet Jordan<sup>1</sup>, Hannah C. Wise<sup>1,4</sup>, Tripti Shrestha Bhattarai<sup>1,2</sup>, Wenhao Hu<sup>1</sup>, Madeline Dorso<sup>1</sup>, James A. Rodrigues<sup>1</sup>, Kwanghee Kim<sup>1</sup>, Aphrothiti J. Hanrahan<sup>1</sup>, Pedram Razavi<sup>5</sup>, Brett Carver<sup>1,6</sup>, Sarat Chandralapaty<sup>1,5</sup>, Jorge S. Reis-Filho<sup>1,3</sup>, Barry S. Taylor<sup>1,2,7,8</sup>, David B. Solit<sup>1,5,7,8</sup>

<sup>1</sup>Human Oncology and Pathogenesis Program, Memorial Sloan Kettering Cancer Center, New York, New York, USA

<sup>2</sup>Department of Epidemiology and Biostatistics, Memorial Sloan Kettering Cancer Center, New York, New York, USA

<sup>3</sup>Department of Pathology, Memorial Sloan Kettering Cancer Center, New York, New York, USA

<sup>4</sup>Louis V. Gerstner, Jr. Graduate School of Biomedical Sciences, Memorial Sloan Kettering Cancer Center, New York, New York, USA

<sup>5</sup>Department of Medicine, Memorial Sloan Kettering Cancer Center, New York, New York, USA

<sup>6</sup>Department of Surgery, Memorial Sloan Kettering Cancer Center, New York, New York, USA

<sup>7</sup>Marie-Josée and Henry R. Kravis Center for Molecular Oncology, Memorial Sloan Kettering Cancer Center, New York, USA

<sup>8</sup>Weill Medical College of Cornell University, New York, USA

### Abstract

Mutational activation of the PI3 kinase/AKT pathway is among the most common pro-oncogenic events in human cancers. The clinical utility of PI3K and AKT inhibitors has, however, been modest to date. Here, we used CRISPR-mediated gene editing to study the biologic consequences of AKT1 E17K mutation by developing an AKT1 E17K-mutant isogenic system in a *TP53*-null background. AKT1 E17K expression under the control of its endogenous promoter enhanced cell growth and colony formation, but had a paradoxical inhibitory effect on cell migration and invasion. The mechanistic basis by which activated AKT1 inhibited cell migration and invasion was increased E-cadherin expression mediated by suppression of ZEB1 transcription via altered  $\beta$ -catenin subcellular localization. This phenotypic effect was AKT1-specific, as AKT2 activation had the opposite effect, a reduction in E-cadherin expression. Consistent with the opposing effects of AKT1 and AKT2 activation on E-cadherin expression, a pro-migratory effect of AKT1 activation was not observed in breast cancer cells with PTEN loss or expression of an activating

**Corresponding Author:** David B. Solit, MD, Human Oncology and Pathogenesis Program, Memorial Sloan Kettering Cancer Center, Mortimer B. Zuckerman Research Center, 417 E 68<sup>th</sup> St, 8<sup>th</sup> Floor, Room Z-804, New York, NY 10065, USA, Phone: 646.888.2641, solitd@mskcc.org.

\*Contributed equally

*PIK3CA* mutation, alterations which induce the activation of both AKT isoforms. The results suggest that the use of AKT inhibitors in breast cancer patients could paradoxically accelerate metastatic progression in some genetic contexts and may explain the frequent co-selection for *CDH1* mutations in *AKT1* mutated breast tumors.

## Keywords

breast cancer; AKT1; migration; E-cadherin;  $\beta$ -catenin

---

## Introduction

The phosphatidylinositol 3-kinase (PI3K)/AKT signaling pathway regulates a variety of cellular processes including cell proliferation, survival and motility. Somatic mutations in the PI3K/AKT pathway are prevalent across a wide variety of cancer types, which has prompted intensive efforts to develop selective inhibitors of key pathway nodes, including the serine/threonine kinase AKT (1). Three AKT genes encode the three AKT isoforms, *AKT1* (AKT1), *AKT2* (AKT2) and *AKT3* (AKT3). Mutations in AKT are present in a minority of human cancers, with the AKT1 E17K mutation being by far the most common hotspot (2).

While selective PI3 kinase and AKT inhibitors have shown promising anti-tumor effects in molecularly defined populations, their clinical activity has been modest in comparison to inhibitors of other mutationally activated kinases such as EGFR, ALK and BRAF (1,3,4). This limited clinical activity has been ascribed to the difficulties of selectively targeting a single AKT isoform *in vivo*, as the three AKT isoforms have highly homologous catalytic domains which are also similar in structure to kinases in the larger cAMP-dependent protein kinase (AGC) family (5). However, even highly selective allosteric inhibitors of AKT, such as MK-2206, which bind to the pleckstrin homology (PH) domain and lock the kinase in an inactive conformation, have had only limited clinical success to date (6,7).

Evidence has emerged that AKT isoforms have distinct roles during tumor initiation and cancer progression. More specifically, AKT1 has been shown to promote tumor initiation through increased cell survival, whereas activation of AKT2 can enhance cell migration and cancer metastasis (8). While ectopic overexpression of AKT1 E17K in non-transformed breast cells results in activation of AKT substrates such as PRAS40 (9), AKT E17K has not been shown to confer oncogenic phenotypes when expressed at physiologic levels (10). Furthermore, studies in cell line and transgenic mouse models suggest that over-expression of activated AKT1 can, at least in some cellular contexts, paradoxically suppress invasion and metastasis (8,11–19). Whether this paradoxical inhibition of oncogenic phenotypes by activated AKT1 is a contributing factor to the limited therapeutic efficacy observed with AKT inhibitors to date remains unknown.

One hurdle to the development of AKT inhibitors as therapeutic agents for AKT-mutant patients has been the lack of AKT1-mutant preclinical models. To further elucidate the biologic role of mutant AKT1 in promoting cell proliferation and invasion, we generated an isogenic AKT1-mutant breast model using CRISPR/Cas9 gene editing. We discovered that

AKT1 and AKT2 had differential effects on  $\beta$ -catenin transcriptional activity. Activated AKT1 inhibited cell migration through reversal of epithelial-mesenchymal transition (EMT), the mechanistic basis for which was sequestration of  $\beta$ -catenin to the cell membrane leading to decreased ZEB1 transcription and a subsequent increase in E-cadherin expression. Conversely, AKT2 activation increased  $\beta$ -catenin transcriptional activity at the ZEB1 promoter and decreased E-cadherin expression. Taken together, the data provide a mechanistic basis for the differential roles of AKT1 and AKT2 in regulating cancer cell invasion through isoform-selective regulation of  $\beta$ -catenin activity and provide strong rationale for the development of isoform-selective AKT inhibitors as anticancer therapies.

## Materials and Methods

### Cell culture

As previously described (20), MCF-10A cells (ATCC) were cultured in DMEM/F12 media supplemented with 5% horse serum (Gibco Thermo Fisher Scientific), human EGF 20 ng/ml (Sigma Life Science), insulin 10  $\mu$ g/ml (Sigma), hydrocortisone 0.5 mg/ml (Sigma), and cholera toxin 100 ng/ml (Sigma). MCF7 cells (a gift from Dr. J. Lauring) were grown in DMEM F-12 media and HEK293T cells (ATCC) in DMEM. All media, except for MCF-10A medium, contained 10% fetal bovine serum (FBS; Thermo Fisher). All cells were maintained at 37°C with 5% CO<sub>2</sub>. The cell lines were authenticated using short tandem repeat profiling before use. Early passaged cells (10 passages) were used for experiments and cell lines were tested bi-monthly to confirm absence of mycoplasma.

### CRISPR/Cas9-mediated knock-in of AKT1 E17K mutation and knockout of *TP53*, *CDH1*, *AKT1*, *AKT2*, *ZEB1*, and *PTEN*

Our knock-in strategy involved introduction of a double strand break introduced by Cas9/sgRNA in the immediate 3' region of the E17 coding sequence of exon 2 of *AKT1*, and a donor template consisting of the K17 mutation flanked by sequences homologous to the *AKT1* genomic sequence. The [crispr.mit.edu](http://crispr.mit.edu) website was used to design sgRNAs targeting exon 2 of *AKT1*, and the oligos (sequences in Supplementary Table 1) were subcloned into LentiCRISPR v2 (Addgene). The donor carrier lentiviral plasmid, LV-GFP-T, was generated from LV-GFP (Addgene) by removing the 3' part of the U6F promoter using Nde I/Mlu I double digestion, Mung Bean Nuclease blunt-ending, followed by re-ligation. The homology E17K repair template was first PCR amplified from human genomic DNA using KAPA HiFi polymerase (KAPA Biosystems), with 1.0-kbp and 1.4-kbp homologous arms on the left and right sides of the E17 codon. The E17K mutation (GAG -> AAG) and sgRNA-specific PAM alterations were introduced by site directed mutagenesis using Herculase II fusion DNA polymerase (Agilent), and the whole sequence was then subcloned into the EcoR I site of LV-GFP-T to generate the donor template lentiviral plasmid (all PCR primers are listed in Supplementary Table 1). Lentivirus was produced by transfecting lentiviral constructs together with psPAX2 and pMD2.G (Addgene) into HEK293T cells using Lipofectamine 2000 (Life Technologies) as previously described (21). MCF-10A cells were infected with both Cas9/sgRNA and E17K donor template lentiviruses, and pools of transduced cells were screened for the AKT1 E17K mutation by genomic locus PCR/Sanger sequencing or CRISPR-seq (Supplementary Fig 1, PCR primers are listed in the "CRISPR-seq" section). If

the AKT1 E17K mutation was present in the cell pool, that pool was sorted by FACS into single clones which were subsequently expanded, again screened by locus PCR and Sanger sequencing, and then validated by CRISPR-seq, mRNA RT-PCR and by targeted next generation sequencing using the MSK-IMPACT assay (22). CRISPR/Cas9 gene knockouts were carried out as previously described (21), and the sgRNA sequences used are listed in Supplementary Table 1.

### CRISPR-seq

PCR primer pairs were designed to amplify a ~2 kbp genomic sequence surrounding AKT1 E17K, with one primer targeting outside of the CRISPR knock-in template sequence. Nested PCR was then performed to amplify a 202-bp sequence surrounding AKT1 E17K. The PCR product was gel purified and deep sequencing of the amplicon was performed using HiSeq instrumentation. Between 750,000 – 1,000,000 reads were reported and aligned to the reference sequence. The PCR Primers used were:

E17K-Primer-9F: GCCTCCTGTCCATGGTACTC

E17KVali-1R: CCTGGGGTGCCCTACTCTAT

E17K-CRISPR-F: AGGGTCTGACGGGTAGAGTG

E17K-CRISPR-R: GAGAGGCCAAGGGGATACTT

### Cell transfection, cell lysate and nuclear extract preparation, Western blotting

MCF-10A cells were transfected with plasmid DNA using X-tremeGENE HP DNA Transfection Reagent according to manufactures instructions (Roche). A ratio of 1:3 of DNA ( $\mu\text{g}$ ) to Transfection Reagent ( $\mu\text{L}$ ) was used. Cells were lysed in whole cell lysis buffer and Western blot analyses were performed as previously described (23). Antibodies used for Western blotting and plasmids used for transfection are listed in Supplementary Table 2 and 3.

### Proliferation, soft agar assays and drug treatment experiments

Cell viability was determined by trypan blue incorporation using a Vi-CELL XR 2.04 (Beckman Coulter) as previously described (24).  $2 \times 10^4$  cells were initially seeded in 6-well plates at Day 0 in standard or deficient media (no EGF and insulin, reduced 2% horse serum). Cells were incubated for 7 days before being counted. Fold increase of each cell line was calculated by: (cell number on Day 7)/(cell number on Day 0).

For soft agar studies, cells ( $1 \times 10^4$ ) were seeded in 0.33% agar in six well plates on top of a 0.5% agar layer along with drug where relevant. Plates were then incubated at 37°C for three weeks. Before imaging, MTT reagent (ATCC) was added to each well and incubated at 37°C for three hours to stain live cell colonies. Plates were imaged and colonies greater than 200 $\mu\text{m}$  were counted using GelCount (Oxford Optronix).

The AKT inhibitors AZD5363, MK2206, ipatasertib, and the HDAC inhibitor RGFP109 were purchased from Selleck Chemicals. For migration assays, cells were pre-treated with

the AKT inhibitor, or a combination of AKT and HDAC inhibitors in deficient media for 24–48 hrs and then Boyden chamber assays were performed in the presence of the drugs.

### Boyden chamber transwell migration/invasion assay

Assays were conducted in 24-well plates. Cells ( $1-15 \times 10^4$ ), starved in deficient media overnight, were seeded in the upper chamber of a transwell chamber insert (8.0  $\mu\text{m}$ , Corning) in deficient media, and 20–30% FBS was added to the deficient medium outside the insert to serve as a chemoattractant. Invasion assays were performed in chamber inserts coated by 40  $\mu\text{L}$  of Matrigel (Corning). After 24-, 48-, or 72-hr incubation periods, migrated cells were fixed and stained with crystal violet (10%)/formaldehyde (37%) solution, followed by microscopic examination. Five random views were selected to count the migrated cells. Each experiment was repeated independently multiple times.

### mRNA extraction, RT-PCR and qRT-PCR of *CDH1* and *ZEB1* mRNA

Total RNA was extracted from cells using the RNeasy Mini Kit according to the manufacturer's instructions (Qiagen). Two micrograms of total RNA were used per sample for cDNA conversion using oligo-dT primers and the iScript cDNA Synthesis Kit (Bio-Rad). Regular RT-PCR was performed using the Platinum Green Hot Start PCR Master Mix (2X) (Thermo Fisher) and visualized by agarose gel electrophoresis. qRT-PCR was performed using QuantiFast SYBR Green PCR kit (Qiagen) on a ViiA7 Real Time PCR System (Life Technologies).

The following PCR primers were used:

CDH1-cDNA-2F: TGCCCAGAAAATGAAAAAGG

CDH1-cDNA-2R: GTGTATGTGGCAATGCGTTC

ZEB1-cDNA-1F: AAGGGCAAGAAATCCTGGGG

ZEB1-cDNA-1R: ATGACCACTGGCTTCTGGTG

Beta-actin-cDNA-1F: CGTGCGTGACATTAAGGAGA

Beta-actin-cDNA-2R: TGATCCACATCTGCTGGAAG

qPCR primers (Qiagen):

CDH1: Hs\_CDH1\_1\_SG QuantiTect Primer (NM\_004360), QT00080143

ZEB1: RT<sup>2</sup> qPCR Primer Assay for Human ZEB1 (NM\_001128128), PPH01922A-200

Beta-actin: Hs\_ACTB\_1\_SG QuantiTect Primer (NM\_001101), QT00095431

### Generation of lentiviral expression constructs

AKT1 E17K mutant was generated by performing site-directed mutagenesis on WT AKT1 (cloned into gateway donor vector pDONR223) using KAPA HiFi polymerase (KAPA Biosystems) and verified by Sanger sequencing. Verified AKT1 E17K coding sequence

(without the stop codon) was sub-cloned into gateway lentiviral vector pLX302 so the V5 tag at C-terminus was expressed in frame with AKT1 cDNA sequence. LR Clonase II enzyme mix (Thermo Fisher Scientific) was used for sub-cloning purpose. PIK3CA E545K mutant cDNA (Cat#RC400348), purchased from OriGene, was inserted into the AsiS I and Mlu I sites of plasmid Lenti-C-Myc-DDK-IRES-Neo (Cat#PS100081, OriGene), to generate PIK3CA-E545K lentiviral expression vector.

### Immunofluorescence

Cells were cultured on Millicell EZ 8-well glass slides (Millipore Sigma) and fixed with 4% paraformaldehyde diluted in phosphate-buffered saline (PBS) at room temperature (RT) for 10 minutes. Cells were then washed three times with PBS before being permeabilized with either ice-cold 100% methanol for 10 minutes at  $-20^{\circ}\text{C}$  or 0.2% Triton X-100 diluted in PBS for 10 minutes at RT. After one wash with PBS, cells were blocked in buffer containing 5% normal goat serum and 0.3% Triton X-100 for 1 hr at RT. Cells were then incubated overnight at  $4^{\circ}\text{C}$  in primary antibodies diluted in PBS with 1% BSA and 0.3% Triton X-100 (Dilution Buffer). After three washes with PBS, cells were incubated in secondary antibodies in Dilution Buffer for 1 hr at RT in the dark. Cells were then rinsed three times with PBS, stained with DAPI for 10 minutes at RT and mounted with Mowiol mounting media. Cells were imaged with MIRAX SCAN.

### Chromatin immunoprecipitation assays (ChIP)

ChIP assays were conducted using a SimpleChIP Enzymatic Chromatin IP kit [Cell Signaling Technologies (CST)]. Parental, p53ko and p53ko/E17K MCF-10A cells were grown to 90% confluence followed by cross-linking with 1% formaldehyde for 10 minutes at RT. Chromatin fragmentation was performed by nuclease digestion and sonication. Chromatin IP was then performed with rabbit monoclonal anti- $\beta$ -catenin antibody (5  $\mu\text{g}$ , Cat#8480, CST), rabbit anti-histone H3 (a technical positive control; 1:50) (Cat#4620, CST), and normal rabbit IgG (a negative control; 5  $\mu\text{g}$ ) (Cat#SC-2027, SCBT). After reverse crosslinking and DNA purification using columns (Cat#28106, Qiagen), immunoprecipitated DNA was amplified by Platinum Green Hot Start PCR Master Mix (2X) (Thermo Fisher), as then quantified by real-time qPCR using the QuantiFast SYBR Green PCR kit (Qiagen). The primers for  $\beta$ -catenin binding sites in the *ZEB1* promoter were (25):

forward primer 5' - GCCGCCGAGCCTCCAACCTT-3',

reverse primer 5' - TGCTAGGGACCGGGCGGTTT-3'.

The positive control primers for the RPL30 exon 3 were from the kit (Cat#7014, CST). Pull-down fold enrichment was calculated based on the threshold cycle (Ct) values normalized by DNA input and negative control IgG values.

### Co-immunoprecipitation assay (Co-IP)

Co-IP was performed as previously described (23). In brief, cells were first lysed in IP buffer [20 mM Tris (pH 7.5), 150 mM NaCl, 1 mM EDTA, 1 mM EGTA, 2.5 mM Sodium pyrophosphate, 1 mM  $\beta$ -glycerophosphate, 1 mM  $\text{Na}_3\text{VO}_4$  and proteinase and phosphatase



inhibitors] without detergent, followed by preclearing using control rabbit or mouse IgG and protein A and GammaBind G Sepharose beads (1:1 protein A/G beads, GE Healthcare). Co-IP was performed by incubating 500 µg of precleared protein extract with 2 µg of antibody and protein A/G beads overnight at 4°C. The beads were washed 5 times with IP buffer before boiling in sample loading buffer and being subjected to Western blot analysis.

## Statistics

All data are represented as means  $\pm$  standard error of the mean (SEM). Student's *t* test (2-tailed) and 1-way ANOVA followed by Tukey post-hoc analysis were used to test for statistical significance.

## Results

### Generation of AKT1 E17K mutant cells

To investigate the biologic role of AKT1 E17K mutation on breast cancer development and progression, we sought to generate AKT1 E17K mutant isogenic cells using a CRISPR knock-in approach (Supplementary Figure 1A, B). As a large proportion of ER-negative breast cancers with AKT1 E17K have co-occurrent mutations in the *TP53* gene (26) (Supplementary Figure 2), we chose to model this combination of mutations in non-transformed, ER-negative MCF-10A human mammary epithelial cells (27). We first performed targeted homozygous inactivation (knock out: "KO") of *TP53* using CRISPR/Cas9 (Supplementary Figure 3), followed by AKT1 E17K knock-in, thereby generating p53ko/AKT1 E17K MCF-10A cells (p53ko/E17K). We subsequently confirmed that the knock-in cells had a heterozygous AKT1 E17K configuration by Sanger sequencing, locus-specific deep sequencing (CRISPR-Seq), and RT-PCR (Supplementary Figure 1C). Furthermore, targeted deep sequencing of 468 cancer-associated genes (MSK-IMPACT) confirmed that with the exception of the engineered *TP53* and *AKT1* mutations, the parental MCF-10A, p53ko, and p53ko/E17K lines had nearly identical genetic backgrounds (data not shown).

### AKT1 E17K mutation induces anchorage-independent growth in a p53-null background

While ectopic overexpression of AKT1 E17K has been shown previously to induce transformation, AKT1 E17K expression at physiologic levels using a homologous recombination knock-in approach in human breast MCF-10A cells did not confer growth factor independence and colony formation in soft agar (2,9,10,28,29). These results suggested that amplification of the mutant allele or additional molecular alterations were needed for the oncogenic effects of AKT1 E17K to manifest (10). We thus examined the effects of AKT1 E17K expression on AKT pathway activation and cellular proliferation in p53ko/E17K cells. In both growth factor-rich culture media (regular media) and EGF and insulin absent media (deficient media), p53ko/E17K cells exhibited a modest increase in phosphorylated AKT (pT308 and pS473) as compared to parental and p53ko cells (Figure 1A). While AKT1 E17K knock-in had minimal effect on steady state levels of downstream AKT effectors including PRAS40 and GSK-3 $\alpha/\beta$ , the activation of PRAS40 and GSK-3 $\alpha/\beta$  were AKT-dependent in the p53ko/E17K cells as shown by a significant decrease in the expression of phosphorylated PRAS40 and GSK-3 $\alpha/\beta$  upon treatment with AZD5363, an

ATP-competitive, pan-AKT kinase inhibitor (Supplementary Figure 4 and data not shown). Furthermore, while we noted only modest increase in the basal expression of p308-AKT in the AKT1 knock-in cells, we did observe a significant change in p308-AKT sub-cellular localization. Immunofluorescence staining revealed that phosphorylated AKT was localized to the plasma membrane in the p53ko/E17K cells whereas it was primarily cytosolic in the AKT1-wildtype p53ko cells (Figure 1B). A similar increase in membranous localization of phosphorylated AKT was also observed in MCF-10A cells engineered to express AKT1 E17K through lentiviral infection (Supplementary Figure 5).

We next assessed the effect of AKT1 E17K on cellular proliferation in the isogenic cell line models. As others have observed, we noted a decrease in proliferation of p53ko cells as compared to parental MCF-10A cells in fully supplemented media conditions (30) (Figure 1C). However, in cells with co-mutation of AKT1 E17K (p53ko/E17K), cell growth was restored to levels greater than that of parental MCF-10A cells (Figure 1C). Notably, only p53ko/E17K cells grew in growth factor-deficient media (absence of EGF and insulin), a cardinal feature of transformed cells (Figure 1C).

The ability to grow in an anchorage-independent manner is also a characteristic of transformed cells and only the p53ko/E17K cells could form colonies in soft agar (Figure 1D). Furthermore, while p53ko/E17K cells were not more sensitive to AKT inhibitors (ADZ5363 and MK2206) than cells with p53ko alone when grown in 2-D culture conditions (Supplementary Figure 6), treatment with the AKT inhibitor AZD5363 abrogated the ability of p53ko/E17K cells to form colonies in soft agar (Figure 1D). Taken together, these results demonstrate that AKT1 E17K expression can confer oncogenic phenotypes to non-transformed, human mammary epithelial cells when expressed at physiological levels under the control of its endogenous promoter in the context of p53 loss-of-function. The oncogenic effects of AKT1 E17K were, however, most apparent when cells were grown in either growth factor deficient or 3D culture conditions.

### **AKT1 E17K mutation restores E-cadherin expression and inhibits cell migration and invasion in a p53 null context**

To investigate whether AKT1 E17K promotes cancer progression through enhanced invasion or migration, we performed transwell migration and invasion assays using the MCF-10A isogenic cells. Consistent with prior studies, p53 loss significantly enhanced migratory and invasive potential (Figure 2A, p53ko), likely due to de-repression of the transcription of cell motility-promoting genes (31,32). We did observe, however, that p53ko/E17K cells had significantly reduced migration and invasion potential as compared to p53ko cells. As increased tumor cell migration, invasiveness, and metastatic potential are often associated with epithelial-to-mesenchymal transition (EMT), we investigated the expression levels of EMT markers in the isogenic cell lines. As compared to parental MCF-10A cells, p53ko cells had increased expression of the EMT markers N-cadherin, ZEB1, and Snail, as well as loss of E-cadherin, which together indicated the acquisition of an EMT phenotype upon p53 loss-of-function (Figure 2B). Notably, the loss of E-cadherin was observed in multiple p53ko MCF-10A cell clones developed separately using different p53 targeting CRISPR sgRNAs, confirming that this phenotype was attributable to loss of p53 function



(Supplementary Figure 3). While several EMT markers remained elevated in p53ko/E17K cells, expression of AKT1 E17K was associated with restoration of E-cadherin expression and downregulation of ZEB1 (Figure 2B). While p53 can also induce MDM2-mediated Slug protein degradation in lung cancer cells (33), p53 knockout in our model resulted in a modest decrease in Slug protein expression, which was not affected by expression of AKT1 E17K (Figure 2B).

As regulation of cell migration by E-cadherin is associated with changes in its subcellular localization, we performed immunofluorescence of E-cadherin in the isogenic cell lines. Consistent with the immunoblot results, p53ko was associated with loss of E-cadherin expression whereas AKT1 E17K knock-in was sufficient to restore E-cadherin expression and its membrane localization in a p53-null context (Figure 2C). We next performed quantitative reverse transcription PCR (RT-qPCR), which revealed that AKT1 E17K knock-in was sufficient to partially restore expression of *CDH1* mRNA in the setting of p53 knockout (Figure 2D). Finally, to establish that restoration of E-cadherin was sufficient to repress cell migration, we infected p53ko/E17K MCF-10A cells with a *CDH1* targeting CRISPR/Cas9 lentivirus. The resulting reduction of E-cadherin level in the resultant cell pool was associated with significantly enhanced cell mobility (Figure 2E).

We further confirmed that *CDH1* gene transcription was AKT1-dependent, by infecting p53ko/E17K cells with an AKT1-targeted CRISPR/Cas9 lentivirus. Reduced AKT1 expression resulted in decreased E-cadherin expression and induction of cell migration in p53ko/E17K cells (Figure 2F). Lastly, to confirm that expression of activated AKT1 was sufficient to restore E-cadherin protein levels in p53ko cells, FLAG-tagged Myr-AKT1, a constitutively activated form of AKT1, was expressed following knockdown of endogenous AKT1 in p53ko cells. Expression of Myr-AKT1 was indeed sufficient to induce E-cadherin expression (Figure 2G). Taken together, the data indicate that the expression of AKT1 E17K can abrogate the enhanced migratory/invasive phenotype induced by *TP53* inactivation in breast cancer cells by inducing E-cadherin expression. The data further suggest that in some co-mutational contexts, AKT1 E17K may paradoxically delay rather than enhance metastatic progression, a phenotype that could be abrogated by co-mutation of *CDH1*, a common co-occurring event in human breast cancers (Supplementary Figure 2).

### **Activated AKT1, but not AKT2, restores E-cadherin expression by inhibiting $\beta$ -catenin/ZEB1 signaling**

Activated AKT1 has been linked to an anti-migratory phenotype through several putative mechanisms including decreased levels of the transcription factor NFAT1, the mTOR pathway effector TSC2, the EMT factor Twist, focal adhesion factors  $\beta$ 1-integrin and phosphorylated FAK, increased ERK pathway signaling and upregulation of the actin-associated protein paladin (8,12–14,18,34). However, we found that none of these potential regulators of cell invasion were differentially altered in p53ko/E17K versus p53ko cells (Supplementary Figure 7). As we were unable to recapitulate prior postulated mechanisms whereby AKT1 activation could impair cell migration and invasion, we sought to define the mechanism whereby AKT1 E17K induced E-cadherin expression in our model. First, we assessed the methylation status of CpG islands in the *CDH1* promoter in each of the cell

lines but noted minimal difference in *CDHI* promoter methylation among the p53ko, p53ko/E17K, and parental MCF-10A cells (Supplementary Figure 8). Next, we analyzed transcription factors that have been shown in some contexts to target and repress transcription of the *CDHI* gene, thereby abrogating E-cadherin expression and promoting EMT (35,36). One such transcription factor is the zinc finger-containing protein ZEB1 (37,38), and we observed that loss of E-cadherin expression in p53ko cells was associated with increased ZEB1 protein expression (Figure 2B). This increased ZEB1 protein expression was accompanied by significantly higher ZEB1 mRNA expression, as determined by RNA-seq (data not shown) and confirmatory RT-qPCR (Figure 3A). ZEB1 and E-cadherin profiles were largely reversed following AKT1 E17K knock-in, with p53ko/E17K cells exhibiting low levels of ZEB1 and high E-cadherin mRNA and protein expression similar to that of parental MCF-10A cells (Figure 2B, D and 3A). Furthermore, ZEB1 loss via CRISPR/Cas9 targeting was sufficient to restore E-cadherin expression in p53ko MCF-10A cells (Figure 3B). In sum, in breast cells with p53 loss-of-function, expression of AKT1 E17K reduced ZEB1 expression, which resulted in increased E-cadherin expression and a reduction in EMT. Notably, this result may explain the shorter disease-free survival observed in breast cancer patients whose tumors exhibit elevated ZEB1 expression (39).

As  $\beta$ -catenin has been hypothesized to be a primary regulator of ZEB1 transcription and one of the key regulators of EMT in breast cancer and other cancer types (40), we sought to explore the functional interaction between AKT1 E17K and ZEB1/E-cadherin signaling. Inactive  $\beta$ -catenin associates with E-cadherin at the cellular membrane, but upon its phosphorylation at Ser552 by AKT and other kinases such as PKA and MSK1,  $\beta$ -catenin translocates to the nucleus, binding to promoter sequences where it co-transactivates target genes such as ZEB1 (41–45). We therefore used immunofluorescence to examine the cellular localization of pS552- $\beta$ -catenin, the transcriptionally active form of  $\beta$ -catenin, in our isogenic system. In p53 null cells, total  $\beta$ -catenin protein levels were lower than that of parental cells, and pS552- $\beta$ -catenin had a predominantly nuclear rather than membrane-bound localization (Figure 2B and Figure 3C). However, in the p53ko/E17K cells, pS552- $\beta$ -catenin sub-cellular localization shifted from the nucleus to the plasma membrane, a localization pattern similar to that of the parental MCF-10A cells (Figure 3C).

As  $\beta$ -catenin is a transcriptional activator, we used chromatin immunoprecipitation (ChIP) to determine whether its binding to the ZEB1 promoter was affected by AKT1 E17K expression. As predicted, and in agreement with the immunofluorescence nuclear localization data, there was increased  $\beta$ -catenin association with the ZEB1 promoter in p53ko cells as compared to parental MCF-10A and p53ko/E17K cells (Figure 3D). These data led us to hypothesize that membranous AKT1 E17K may regulate ZEB1 by binding to and sequestering  $\beta$ -catenin at the cell membrane, thus preventing its entry into the nucleus, thereby impairing its ability to induce ZEB1 transcription and subsequent E-cadherin loss. We thus performed reciprocal co-immunoprecipitation assays using either a  $\beta$ -catenin or AKT1 antibody. Notably, more AKT1 was bound to  $\beta$ -catenin in parental and p53ko/E17K cells than in p53ko cells (Figure 3E). Interestingly, E-cadherin was also bound to  $\beta$ -catenin in parental cells, but this association was lost in p53ko and p53ko/E17K cells (Figure 3E). These data suggest that AKT1 E17K, and not the canonical E-cadherin, is sequestering  $\beta$ -

Author Manuscript

catenin at the cellular membrane in p53ko/E17K cells (46). The findings imply that the restoration of E-cadherin expression upon AKT1 E17K mutation may be secondary to a change in  $\beta$ -catenin localization. To map the  $\beta$ -catenin binding region within AKT1, we expressed in 293T cells FLAG-tagged  $\beta$ -catenin and HA-tagged full length AKT or one of three fragments of AKT1: PH domain only (aa1–149), kinase domain only (aa120–433), and a fragment containing the PH and kinase domains but lacking the c-terminal hydrophobic motif (aa 1–408) (see Supplementary Figure 9A). Co-immunoprecipitation studies indicated that  $\beta$ -catenin interacted with the full-length HA-tagged AKT1 and the two AKT1 fragments containing the kinase domain but not the fragment containing only the PH domain (Supplementary Figure 9B).

Author Manuscript

As previous studies have suggested that AKT isoforms may function differently during tumorigenesis and metastasis, we next sought to determine whether the effect of AKT1 on E-cadherin expression and thus cell migration and invasion was AKT isoform specific (8,34). We thus measured AKT1- and AKT2-specific phosphorylation levels in each of the isogenic cell lines. Immunoprecipitation data showed that AKT1 phosphorylation was proportionally higher in the p53ko/E17K cells than in p53ko cells. Interestingly, AKT2 phosphorylation was higher in p53ko cells than in p53ko/E17K cells, implying that expression of E17K AKT1 may result in a reduction in AKT2 phosphorylation (Figure 3E). To directly test this possibility, we ectopically expressed AKT1 E17K in MCF-10A cells and found that expression of phosphorylated AKT2 was significantly reduced following AKT1 E17K lentiviral infection, suggesting that AKT1 activation results in reciprocal inactivation of AKT2 (Supplementary Figure 10).

Author Manuscript

The above data led us to postulate that the ratio of activated AKT1/AKT2 may dictate the localization of  $\beta$ -catenin and the subsequent transactivation of ZEB1. To test this hypothesis, we knocked down the expression of AKT1 using CRISPR/Cas9 in p53ko/E17K cells and quantified binding of  $\beta$ -catenin to the ZEB1 promoter by ChIP (Figure 4A). AKT1 knockdown was associated with an increase in association between  $\beta$ -catenin and the ZEB1 promoter in p53ko/E17K cells. Conversely,  $\beta$ -catenin binding to the ZEB1 promoter was decreased when AKT2 was knocked down by CRISPR/Cas9 in p53ko cells (Figure 4A). In sum, the data suggest that AKT1 and AKT2 have opposing effects on the binding of  $\beta$ -catenin to the ZEB1 promoter in breast cells.

Author Manuscript

In order to discern whether AKT2 activation was sufficient to decrease E-cadherin protein levels, Myr-AKT2 (activated AKT2) was expressed in p53ko/E17K cells. In contrast to Myr-AKT1, expression of Myr-AKT2 caused a reduction in E-cadherin protein levels (Figure 4B). To confirm that the suppressive effect of AKT2 on E-cadherin protein levels was not unique to MCF-10A cells, Myr-AKT2 was expressed in MCF7 breast cancer cells following gene-targeted correction of the PIK3CA E545K mutation back to wild-type (47). Interestingly, in both cell lines, the reduction in E-cadherin levels (64–79% reduction) following expression of Myr-AKT2 was reversed upon co-expression of Myr-AKT1 (Figure 4B, last lanes). Conversely, we observed a small increase of E-cadherin when AKT2 was depleted via CRISPR/Cas9 from p53ko cells, which was significantly enhanced following ectopic expression of either Myr-AKT1 or AKT1 E17K (Supplementary Figure 11). Finally, neither *PTEN* loss via CRISPR-mediated knockdown nor expression of an activating

*PIK3CA* mutant (E545K), alterations capable of activating both AKT1 and AKT2, altered E-cadherin levels (Figure 4C). These data suggest that the increase in *CDH1* expression observed in the AKT1 knock-in cells was AKT1-specific. Taken together, the data indicate that AKT1 and AKT2 have opposing effects on cell migration and invasion through regulation of  $\beta$ -catenin transcriptional activity which in turn dictates E-cadherin expression levels (Supplementary Figure 12).

### AKT kinase inhibition can paradoxically enhance cell migration in AKT1 E17K cells

As the AKT1 E17K mutation induced E-cadherin expression by suppressing  $\beta$ -catenin/ZEB1 transcriptional activity in breast cells, we hypothesized that treatment with AKT kinase inhibitors could, in some cellular contexts, increase cell migration by reducing E-cadherin expression. To test this hypothesis, we treated the isogenic MCF-10A cell lines with the ATP competitive, pan-AKT inhibitor AZD5363, which has modestly greater potency for AKT1 than AKT2 (IC<sub>50</sub> 3 vs 7 nM) as well as high potency toward AKT1 E17K based on cell viability assays (48). We then measured the migration of each of the isogenic cell lines using transwell assays. As predicted, treatment with AZD5363 promoted cell migration, modestly in MCF-10A parental cells and to a significantly greater degree in p53ko/E17K cells (Figure 5A). Treatment of p53ko/E17K cells with ipatasertib (49), an ATP competitive AKT kinase inhibitor (IC<sub>50</sub>s: AKT1 5 and AKT2 18 nM) also resulted in increased cell migration (data not shown). These results suggest that the use of AKT inhibitors in patients with breast cancer could paradoxically accelerate metastatic progression in some genetic contexts. As ZEB1 directly interacts with HDAC1/2 to recruit the HDAC1/2-associated repressor complex to the *CDH1* promoter resulting in a silencing of E-cadherin expression (38), we tested whether HDAC inhibition could antagonize the pro-migratory effect of AKT inhibition in AKT1 E17K expressing cells. As predicted, co-treatment with the HDAC inhibitor RGFP109 abrogated the cell migration induced by AZD5363 inhibition in p53ko/E17K cells (Figure 5B).

## Discussion

Despite the high prevalence of PI3 kinase/AKT pathway activation in human cancers, AKT inhibitors have demonstrated only modest clinical activity to date. While AKT inhibitors have demonstrated limited clinical activity in tumors with PTEN loss or PI3 kinase mutation, the alpha selective PI3 kinase inhibitor alpelisib was recently FDA-approved for use in combination with the selective estrogen receptor degrader fulvestrant in *PIK3CA*-mutant breast cancer patients (50). A histology-agnostic basket study of the pan-AKT kinase inhibitor AZD5363 also demonstrated promising anti-tumor activity in patients with breast and endometrial cancers whose tumors harbored AKT1 E17K mutation (3). These results indicate that optimal use of PI3K/AKT pathway inhibitors will require a better understanding of the biologic mechanisms whereby alterations in this pathway induce transformation and cancer progression.

To explore in depth the biologic consequences of AKT1 mutation, we developed an AKT1 E17K isogenic cell line model through CRISPR-mediated knock-in of the E17K mutation into the endogenous *AKT1* gene locus. While AKT1 E17K had modest effects on cell

growth in fully supplemented media, AKT1 E17K knock-in significantly enhanced cells growth in deficient media conditions and colony formation in soft agar. Despite these growth promoting effects of AKT1 E17K, cells expressing AKT1 E17K cells had reduced migratory and invasive capacity suggesting that in some co-mutational contexts such as *TP53* mutation, expression of AKT1 E17K could impair metastatic progression.

Consistent with previous studies in non-transformed and transformed cell line systems, we observed that expression of the cell adhesion molecule E-cadherin was markedly decreased following p53 knockout (51–54). Conversely, expression of AKT1 in *TP53*-null breast cells was sufficient to restore E-cadherin expression and paradoxically inhibit cell migration and invasion. Our data thus provide a mechanistic explanation for the frequent co-selection for loss-of-function *CDH1* mutations in AKT1 E17K-mutant tumors. It was recently demonstrated that breast cancer cells lacking E-cadherin have greater invasive potential but survive poorly *in vivo* and thus ultimately metastasize at a lower efficiency due to increased apoptosis (55). Our findings suggest that *AKT1* mutation while impairing invasion in an E-cadherin wildtype context may cooperate with E-cadherin loss by abrogating the diminished survival observed in highly invasive E-cadherin negative cells.

Exploration of the mechanistic basis by which p53 and AKT1 E17K regulate E-cadherin revealed that loss of p53 resulted in increased expression of the transcription factor ZEB1, whereas AKT1 E17K mutation was sufficient to suppress ZEB1 transcription in a *TP53* null context. Transcription of ZEB1 has been shown to be activated by nuclear accumulation of  $\beta$ -catenin, and both AKT1 and AKT2 can phosphorylate  $\beta$ -catenin at Ser552 resulting in increased nuclear translocation of  $\beta$ -catenin and transcription of  $\beta$ -catenin-associated genes (41,42). Co-immunoprecipitation and immunofluorescence studies, indicated that  $\beta$ -catenin bound to the kinase catalytic domain of AKT1, and expression of AKT1 E17K increased the plasma membrane localization of AKT1 (i.e. the E17K mutation is in the membrane-localized PIP3 binding PH domain) resulting in retention of  $\beta$ -catenin on the cellular membrane and a reduction in  $\beta$ -catenin transcriptional activity on the ZEB1 promoter as shown in Supplementary Figure 12. Myristolated AKT1 could also induced E-cadherin expression, indicating that this mechanism was not specific to the E17K mutation. The effect was, however, AKT isoform selective as expression of an activated AKT2 produced the opposite phenotype, a reduction in E-cadherin expression. Of note, quantification analyses indicated that E-cadherin levels were reduced by only 64–79% following expression of AKT2 suggesting that E-cadherin expression is not exclusively regulated by the two AKT isoforms in breast cancer cells. AKT1 and AKT2 also had opposing effects on the binding of  $\beta$ -catenin to the ZEB1 promoter. Our study thus reveals a novel biologic difference among the AKT1 and AKT2 isoforms, specifically, opposing roles in the regulation of Wnt/ $\beta$ -catenin signaling.

While AKT1 and AKT2 have previously been shown to have opposing effects on tumor induction and migration, we were unable to corroborate previously postulated roles for NFAT, palladin, ERK, TSC2, Twist1,  $\beta$ 1-integrin and FAK as mediators of this phenotype. One possibility is that we expressed AKT1 at physiologic levels under the control of its endogenous promoter whereas prior studies relied on overexpression models. Cell lineage-specific differences in the regulation of E-cadherin could also account for our inability to

validate previously postulated mechanisms of enhanced cell migration by activated AKT1. For example, Kircher *et al.* reported that AKT1 E17K promoted brain metastasis in an autochthonous mouse model of cutaneous melanoma by increasing migration and invasion of melanoma cells (56). This effect was, however, observed in the background of Cre-mediated expression of BRAF<sup>V600E</sup>, and loss of *Cdkn2a* and *Pten*.

While mutations in AKT1 are less prevalent in breast cancer as compared to activating *PIK3CA* mutations (~30%) or PTEN loss (~10–40%), the mutual exclusivity of these genetic alterations suggests they have considerable functional overlap. The anti-invasive phenotype of AKT1 E17K demonstrated here may explain in part the relative rarity of AKT1 mutations as compared to *PIK3CA* and *PTEN* alterations. As *PIK3CA* mutation and PTEN loss induce activation of all three AKT isoforms, mutational alterations in these genes did not result in re-expression of E-cadherin or an anti-migratory/invasive phenotype in breast cancer cells.

The results presented here have potential relevance for the development of AKT inhibitors as cancer therapies. The use of selective AKT1 inhibitors in AKT1 E17K-mutant, *CDHI*-wildtype tumor cells could result in increased cell migration. As this pro-oncogenic effect of AKT inhibition is mediated by decreased expression of E-cadherin, co-administration of an HDAC inhibitor was sufficient to prevent AKT inhibitor induced cell migration suggesting a possible rational combination strategy. Future studies will be needed to determine if this phenomenon is lineage specific or observed in cancers arising at other sites.

## Supplementary Material

Refer to Web version on PubMed Central for supplementary material.

## Acknowledgments

This work was supported by the National Institutes of Health (NIH) (R01 CA234361 to S. Chandarlapaty and D.B. Solit, R01 CA207244 and R01 CA204749 to B.S. Taylor), NIH/NCI Cancer Center Support Grant P30 CA008748 (MSKCC), Cycle for Survival (D.B. Solit), the Breast Cancer Research Foundation (S. Chandarlapaty, J.S. Reis-Filho) and the Marie-Josée and Henry R. Kravis Center for Molecular Oncology (D.B. Solit).

Conflict of Interest

P. Razavi reports consulting and being on advisory board for Novartis and receives institutional research support from GRAIL, Inc. S. Chandarlapaty has consulted with/received honoraria from Lilly, Novartis, BMS, Sermonix, Context, Revolution Medicine, and received institutional research funds from Daiichi-Sankyo, Sanofi, Genentech and Novartis. J.S. Reis-Filho has consulted with/received honoraria from Goldman Sachs Merchant Bank, REPARE Therapeutics, and has been Scientific Advisory Board member of Paige.AI, Volition Rx, as well as ad hoc Scientific Advisory Board member of Ventana Medical Systems, Roche Tissue Diagnostics, Roche, Genentech, Novartis and InVivo. B.S. Taylor reports advisory board activities for Boehringer Ingelheim and honoraria and research funding from Genentech. D.B. Solit has consulted with/received honoraria from Pfizer, Loxo Oncology, Lilly Oncology, Illumina, Vivideon Oncology and BridgeBio.

## References

1. Fruman DA, Rommel C. PI3K and cancer: lessons, challenges and opportunities. *Nat Rev Drug Discov* 2014;13:140–56 [PubMed: 24481312]
2. Carpten JD, Faber AL, Horn C, Donoho GP, Briggs SL, Robbins CM, et al. A transforming mutation in the pleckstrin homology domain of AKT1 in cancer. *Nature* 2007;448:439–44 [PubMed: 17611497]



3. Hyman DM, Smyth LM, Donoghue MTA, Westin SN, Bedard PL, Dean EJ, et al. AKT Inhibition in Solid Tumors With AKT1 Mutations. *J Clin Oncol* 2017;35:2251–9 [PubMed: 28489509]
4. Brown JS, Banerji U. Maximising the potential of AKT inhibitors as anti-cancer treatments. *Pharmacol Ther* 2017;172:101–15 [PubMed: 27919797]
5. Pearce LR, Komander D, Alessi DR. The nuts and bolts of AGC protein kinases. *Nat Rev Mol Cell Biol* 2010;11:9–22 [PubMed: 20027184]
6. Jansen VM, Mayer IA, Arteaga CL. Is There a Future for AKT Inhibitors in the Treatment of Cancer? *Clin Cancer Res* 2016;22:2599–601 [PubMed: 26979397]
7. Ma CX, Sanchez C, Gao F, Crowder R, Naughton M, Pluard T, et al. A Phase I Study of the AKT Inhibitor MK-2206 in Combination with Hormonal Therapy in Postmenopausal Women with Estrogen Receptor-Positive Metastatic Breast Cancer. *Clin Cancer Res* 2016;22:2650–8 [PubMed: 26783290]
8. Irie HY, Pearline RV, Grueneberg D, Hsia M, Ravichandran P, Kothari N, et al. Distinct roles of Akt1 and Akt2 in regulating cell migration and epithelial-mesenchymal transition. *J Cell Biol* 2005;171:1023–34 [PubMed: 16365168]
9. Davies BR, Guan N, Logie A, Crafter C, Hanson L, Jacobs V, et al. Tumors with AKT1E17K Mutations Are Rational Targets for Single Agent or Combination Therapy with AKT Inhibitors. *Mol Cancer Ther* 2015;14:2441–51 [PubMed: 26351323]
10. Lauring J, Cosgrove DP, Fontana S, Gustin JP, Konishi H, Abukhdeir AM, et al. Knock in of the AKT1 E17K mutation in human breast epithelial cells does not recapitulate oncogenic PIK3CA mutations. *Oncogene* 2010;29:2337–45 [PubMed: 20101210]
11. Hutchinson JN, Jin J, Cardiff RD, Woodgett JR, Muller WJ. Activation of Akt-1 (PKB-alpha) can accelerate ErbB-2-mediated mammary tumorigenesis but suppresses tumor invasion. *Cancer Res* 2004;64:3171–8 [PubMed: 15126356]
12. Liu H, Radisky DC, Nelson CM, Zhang H, Fata JE, Roth RA, et al. Mechanism of Akt1 inhibition of breast cancer cell invasion reveals a protumorigenic role for TSC2. *Proc Natl Acad Sci U S A* 2006;103:4134–9 [PubMed: 16537497]
13. Yoeli-Lerner M, Yiu GK, Rabinovitz I, Erhardt P, Jauliac S, Toker A. Akt blocks breast cancer cell motility and invasion through the transcription factor NFAT. *Mol Cell* 2005;20:539–50 [PubMed: 16307918]
14. Chin YR, Toker A. The actin-bundling protein palladin is an Akt1-specific substrate that regulates breast cancer cell migration. *Mol Cell* 2010;38:333–44 [PubMed: 20471940]
15. Ooms LM, Binge LC, Davies EM, Rahman P, Conway JR, Gurung R, et al. The Inositol Polyphosphate 5-Phosphatase PIPP Regulates AKT1-Dependent Breast Cancer Growth and Metastasis. *Cancer Cell* 2015;28:155–69 [PubMed: 26267533]
16. Arboleda MJ, Lyons JF, Kabbinnar FF, Bray MR, Snow BE, Ayala R, et al. Overexpression of AKT2/protein kinase Bbeta leads to up-regulation of beta1 integrins, increased invasion, and metastasis of human breast and ovarian cancer cells. *Cancer Res* 2003;63:196–206 [PubMed: 12517798]
17. Maroulakou IG, Oemler W, Naber SP, Tschlis PN. Akt1 ablation inhibits, whereas Akt2 ablation accelerates, the development of mammary adenocarcinomas in mouse mammary tumor virus (MMTV)-ErbB2/neu and MMTV-polyoma middle T transgenic mice. *Cancer Res* 2007;67:167–77 [PubMed: 17210696]
18. Li CW, Xia W, Lim SO, Hsu JL, Huo L, Wu Y, et al. AKT1 Inhibits Epithelial-to-Mesenchymal Transition in Breast Cancer through Phosphorylation-Dependent Twist1 Degradation. *Cancer Res* 2016;76:1451–62 [PubMed: 26759241]
19. Peng Z, Weber JC, Han Z, Shen R, Zhou W, Scott JR, et al. Dichotomy effects of Akt signaling in breast cancer. *Mol Cancer* 2012;11:61 [PubMed: 22917467]
20. Debnath J, Muthuswamy SK, Brugge JS. Morphogenesis and oncogenesis of MCF-10A mammary epithelial acini grown in three-dimensional basement membrane cultures. *Methods* 2003;30:256–68 [PubMed: 12798140]
21. Al-Ahmadie HA, Iyer G, Lee BH, Scott SN, Mehra R, Bagrodia A, et al. Frequent somatic CDH1 loss-of-function mutations in plasmacytoid variant bladder cancer. *Nat Genet* 2016;48:356–8 [PubMed: 26901067]

22. Zehir A, Benayed R, Shah RH, Syed A, Middha S, Kim HR, et al. Mutational landscape of metastatic cancer revealed from prospective clinical sequencing of 10,000 patients. *Nat Med* 2017;23:703–13 [PubMed: 28481359]
23. Gao SP, Chang Q, Mao N, Daly LA, Vogel R, Chan T, et al. JAK2 inhibition sensitizes resistant EGFR-mutant lung adenocarcinoma to tyrosine kinase inhibitors. *Sci Signal* 2016;9:ra33 [PubMed: 27025877]
24. Hanrahan AJ, Schultz N, Westfal ML, Sakr RA, Giri DD, Scarperi S, et al. Genomic complexity and AKT dependence in serous ovarian cancer. *Cancer Discov* 2012;2:56–67 [PubMed: 22328975]
25. Cieply B, Farris J, Denvir J, Ford HL, Frisch SM. Epithelial-mesenchymal transition and tumor suppression are controlled by a reciprocal feedback loop between ZEB1 and Grainyhead-like-2. *Cancer Res* 2013;73:6299–309 [PubMed: 23943797]
26. Razavi P, Chang MT, Xu G, Bandlamudi C, Ross DS, Vasan N, et al. The Genomic Landscape of Endocrine-Resistant Advanced Breast Cancers. *Cancer Cell* 2018;34:427–38 e6 [PubMed: 30205045]
27. Chavez KJ, Garimella SV, Lipkowitz S. Triple negative breast cancer cell lines: one tool in the search for better treatment of triple negative breast cancer. *Breast Dis* 2010;32:35–48 [PubMed: 21778573]
28. De Marco C, Malanga D, Rinaldo N, De Vita F, Scrima M, Lovisa S, et al. Mutant AKT1-E17K is oncogenic in lung epithelial cells. *Oncotarget* 2015;6:39634–50 [PubMed: 26053093]
29. Guo G, Qiu X, Wang S, Chen Y, Rothman PB, Wang Z, et al. Oncogenic E17K mutation in the pleckstrin homology domain of AKT1 promotes v-Abl-mediated pre-B-cell transformation and survival of Pim-deficient cells. *Oncogene* 2010;29:3845–53 [PubMed: 20440266]
30. Weiss MB, Vitolo MI, Mohseni M, Rosen DM, Denmeade SR, Park BH, et al. Deletion of p53 in human mammary epithelial cells causes chromosomal instability and altered therapeutic response. *Oncogene* 2010;29:4715–24 [PubMed: 20562907]
31. Muller PA, Vousden KH, Norman JC. p53 and its mutants in tumor cell migration and invasion. *J Cell Biol* 2011;192:209–18 [PubMed: 21263025]
32. Powell E, Piwnica-Worms D, Piwnica-Worms H. Contribution of p53 to metastasis. *Cancer Discov* 2014;4:405–14 [PubMed: 24658082]
33. Wang SP, Wang WL, Chang YL, Wu CT, Chao YC, Kao SH, et al. p53 controls cancer cell invasion by inducing the MDM2-mediated degradation of Slug. *Nat Cell Biol* 2009;11:694–704 [PubMed: 19448627]
34. Riggio M, Perrone MC, Polo ML, Rodriguez MJ, May M, Abba M, et al. AKT1 and AKT2 isoforms play distinct roles during breast cancer progression through the regulation of specific downstream proteins. *Sci Rep* 2017;7:44244 [PubMed: 28287129]
35. Huber MA, Kraut N, Beug H. Molecular requirements for epithelial-mesenchymal transition during tumor progression. *Curr Opin Cell Biol* 2005;17:548–58 [PubMed: 16098727]
36. Wong TS, Gao W, Chan JY. Transcription regulation of E-cadherin by zinc finger E-box binding homeobox proteins in solid tumors. *Biomed Res Int* 2014;2014:921564 [PubMed: 25197668]
37. Eger A, Aigner K, Sonderegger S, Dampier B, Oehler S, Schreiber M, et al. DeltaEF1 is a transcriptional repressor of E-cadherin and regulates epithelial plasticity in breast cancer cells. *Oncogene* 2005;24:2375–85 [PubMed: 15674322]
38. Schneider G, Kramer OH, Saur D. A ZEB1-HDAC pathway enters the epithelial to mesenchymal transition world in pancreatic cancer. *Gut* 2012;61:329–30 [PubMed: 22147511]
39. Jang MH, Kim HJ, Kim EJ, Chung YR, Park SY. Expression of epithelial-mesenchymal transition-related markers in triple-negative breast cancer: ZEB1 as a potential biomarker for poor clinical outcome. *Hum Pathol* 2015;46:1267–74 [PubMed: 26170011]
40. Wang Y, Bu F, Royer C, Serres S, Larkin JR, Soto MS, et al. ASPP2 controls epithelial plasticity and inhibits metastasis through beta-catenin-dependent regulation of ZEB1. *Nat Cell Biol* 2014;16:1092–104 [PubMed: 25344754]
41. Sanchez-Tillo E, de Barrios O, Siles L, Cuatrecasas M, Castells A, Postigo A. beta-catenin/TCF4 complex induces the epithelial-to-mesenchymal transition (EMT)-activator ZEB1 to regulate tumor invasiveness. *Proc Natl Acad Sci U S A* 2011;108:19204–9 [PubMed: 22080605]

42. Fang D, Hawke D, Zheng Y, Xia Y, Meisenhelder J, Nika H, et al. Phosphorylation of beta-catenin by AKT promotes beta-catenin transcriptional activity. *J Biol Chem* 2007;282:11221–9 [PubMed: 17287208]
43. Wu S, Wang S, Zheng S, Verhaak R, Koul D, Yung WK. MSK1-Mediated beta-Catenin Phosphorylation Confers Resistance to PI3K/mTOR Inhibitors in Glioblastoma. *Mol Cancer Ther* 2016;15:1656–68 [PubMed: 27196759]
44. Taurin S, Sandbo N, Qin Y, Browning D, Dulin NO. Phosphorylation of beta-catenin by cyclic AMP-dependent protein kinase. *J Biol Chem* 2006;281:9971–6 [PubMed: 16476742]
45. Valenta T, Hausmann G, Basler K. The many faces and functions of beta-catenin. *EMBO J* 2012;31:2714–36 [PubMed: 22617422]
46. Orsulic S, Huber O, Aberle H, Arnold S, Kemler R. E-cadherin binding prevents beta-catenin nuclear localization and beta-catenin/LEF-1-mediated transactivation. *J Cell Sci* 1999;112 ( Pt 8):1237–45 [PubMed: 10085258]
47. Beaver JA, Gustin JP, Yi KH, Rajpurohit A, Thomas M, Gilbert SF, et al. PIK3CA and AKT1 mutations have distinct effects on sensitivity to targeted pathway inhibitors in an isogenic luminal breast cancer model system. *Clin Cancer Res* 2013;19:5413–22 [PubMed: 23888070]
48. Davies BR, Greenwood H, Dudley P, Crafter C, Yu DH, Zhang J, et al. Preclinical pharmacology of AZD5363, an inhibitor of AKT: pharmacodynamics, antitumor activity, and correlation of monotherapy activity with genetic background. *Mol Cancer Ther* 2012;11:873–87 [PubMed: 22294718]
49. Lin J, Sampath D, Nannini MA, Lee BB, Degtyarev M, Oeh J, et al. Targeting activated Akt with GDC-0068, a novel selective Akt inhibitor that is efficacious in multiple tumor models. *Clin Cancer Res* 2013;19:1760–72 [PubMed: 23287563]
50. Andre F, Ciruelos E, Rubovszky G, Campone M, Loibl S, Rugo HS, et al. Alpelisib for PIK3CA-Mutated, Hormone Receptor-Positive Advanced Breast Cancer. *N Engl J Med* 2019;380:1929–40 [PubMed: 31091374]
51. Zhang Y, Yan W, Chen X. Mutant p53 disrupts MCF-10A cell polarity in three-dimensional culture via epithelial-to-mesenchymal transitions. *J Biol Chem* 2011;286:16218–28 [PubMed: 21454711]
52. Chang CJ, Chao CH, Xia W, Yang JY, Xiong Y, Li CW, et al. p53 regulates epithelial-mesenchymal transition and stem cell properties through modulating miRNAs. *Nat Cell Biol* 2011;13:317–23 [PubMed: 21336307]
53. Oikawa T, Otsuka Y, Onodera Y, Horikawa M, Handa H, Hashimoto S, et al. Necessity of p53-binding to the CDH1 locus for its expression defines two epithelial cell types differing in their integrity. *Sci Rep* 2018;8:1595 [PubMed: 29371630]
54. Kim T, Veronese A, Pichiorri F, Lee TJ, Jeon YJ, Volinia S, et al. p53 regulates epithelial-mesenchymal transition through microRNAs targeting ZEB1 and ZEB2. *J Exp Med* 2011;208:875–83 [PubMed: 21518799]
55. Padmanaban V, Krol I, Suhail Y, Szczerba BM, Aceto N, Bader JS, et al. E-cadherin is required for metastasis in multiple models of breast cancer. *Nature* 2019;573:439–44 [PubMed: 31485072]
56. Kircher DA, Trombetti KA, Silvis MR, Parkman GL, Fischer GM, Angel SN, et al. AKT1(E17K) Activates Focal Adhesion Kinase and Promotes Melanoma Brain Metastasis. *Mol Cancer Res* 2019;17:1787–800 [PubMed: 31138602]

**Implications:**

AKT1 E17K mutation in breast cancer impairs migration/invasiveness via sequestration of  $\beta$ -catenin to the cell membrane leading to decreased ZEB1 transcription, resulting in increased E-cadherin expression and a reversal of epithelial-mesenchymal transition.

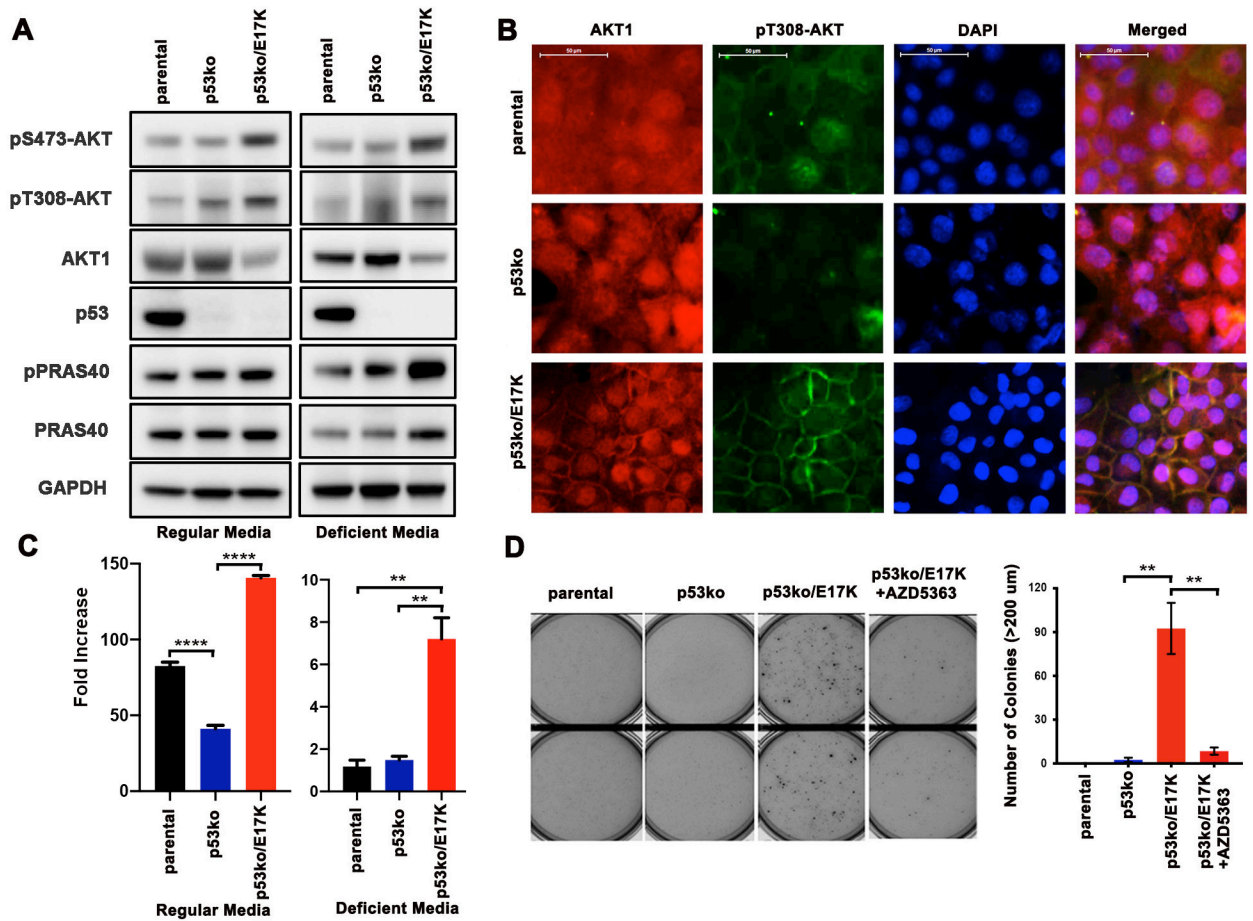


**Figure 1. AKT1 E17K enhances cell proliferation and anchorage independent growth in p53 knockout MCF-10A cells.**

**A**, Western blot of lysates from parental, p53 knockout (p53ko) and p53ko, AKT1 E17K knock-in (p53ko/E17K) MCF-10A cells cultured in regular media and growth factor deficient media. **B**, Immunofluorescence staining of AKT1 and pAKT (T308) in the MCF-10A isogenic cells. Cell nuclei were labeled with DAPI. Scale bar represents 50  $\mu$ m. **C**,  $2 \times 10^4$  cells were plated at Day 0 and cell number was calculated after 7 days of growth in regular or EGF and insulin deficient media. Fold increase for each cell line was defined as (cell number on Day 7)/(cell number on Day 0). Error bars represent mean  $\pm$  SEM (n=3). **D**, Cells were plated in soft agar with or without AZD5363 (3  $\mu$ M) and after 21 days, cell colonies >200  $\mu$ m were counted (right panel). Error bars represent mean  $\pm$  SEM (n=2). The result was repeated and confirmed. *P* values were determined by 1-way ANOVA followed by Tukey post-hoc test. \*\**P*<0.01; \*\*\*\**P*<0.0001.



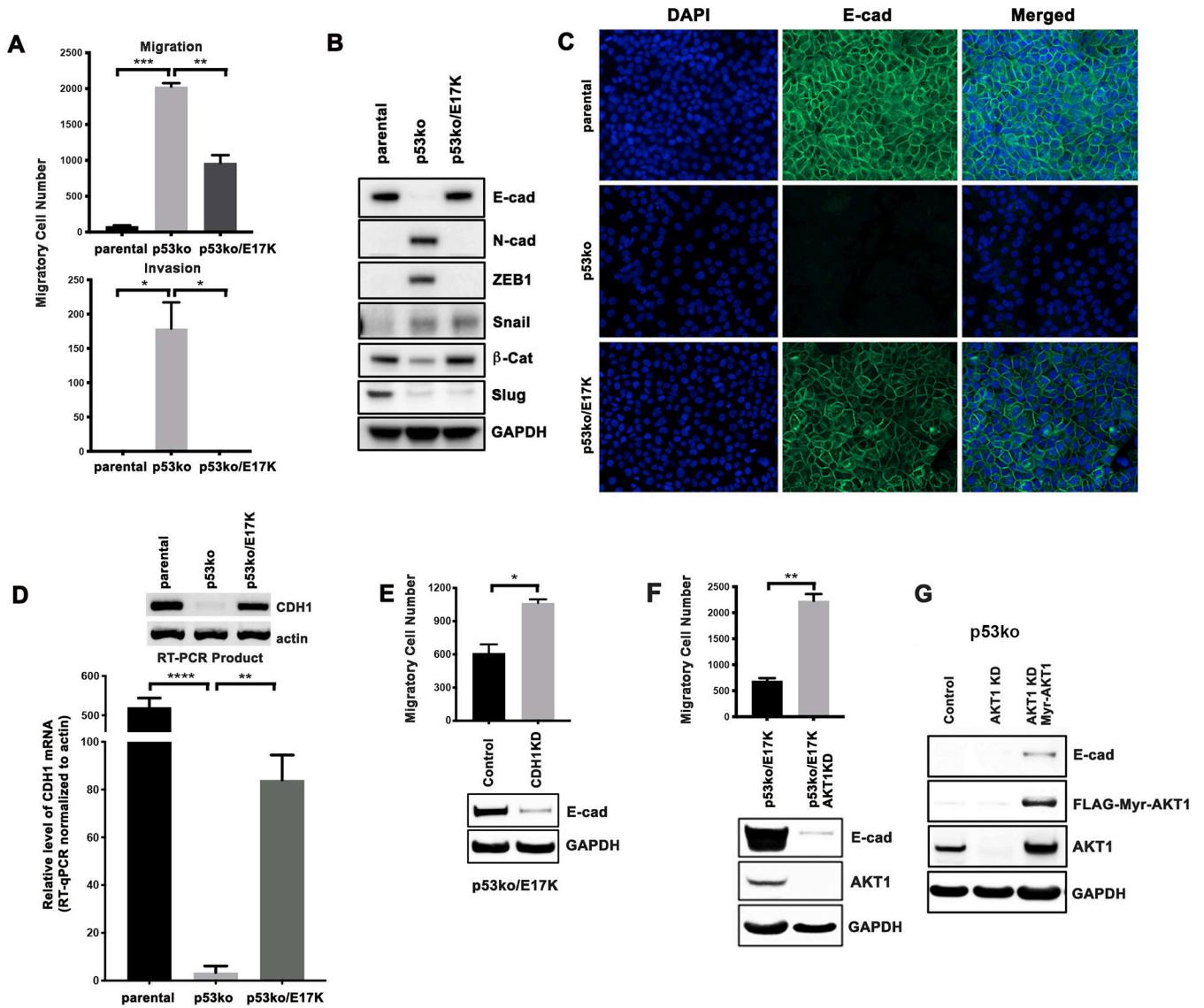


**Figure 2. AKT1 E17K inhibits breast cancer cell migration and invasion by increasing E-cadherin expression.**

**A**, For Boyden chamber assays, cells were plated in a transwell insert for cell migration assays, or a transwell insert with Matrigel coating for cell invasion assays. After 24 hours, migrated/invaded cells were counted. The result was repeated and confirmed. **B**, Western blot of EMT markers from cell lysates. **C**, Immunofluorescence staining of E-cadherin. DAPI staining was performed to identify nuclei. **D**, *CDH1* mRNA levels were determined by RT-qPCR. RT-PCR products were subsequently run on an agarose gel along with actin as control (insert). **E**, p53ko/E17K cells were infected with a CRISPR/Cas9 lentivirus targeting *CDH1* (CDH1KD). Western blot of lysates was performed to confirm E-cadherin knockdown with GAPDH shown as a loading control. Boyden chamber assays were then performed to compare the migration of p53ko/E17K and p53ko/E17K/CDH1KD cells. **F**, Western blot of lysates from MCF-10A p53ko/E17K cells infected with a CRISPR/Cas9 lentivirus targeting *AKT1* (AKT1KD). Boyden chamber migration assays were performed as



in panels **A** and **E. G**, Western blot of lysates from p53ko cells infected with a CRISPR/Cas9 lentivirus targeting *AKT1* followed by expression of FLAG-Myr-AKT1. Error bars represent mean  $\pm$  SEM (n=2 to 3). *P* values were determined by Student's *t* test. \**P*<0.05; \*\**P*<0.01; \*\*\**P*<0.001; \*\*\*\**P*<0.0001.

Author Manuscript

Author Manuscript

Author Manuscript

Author Manuscript

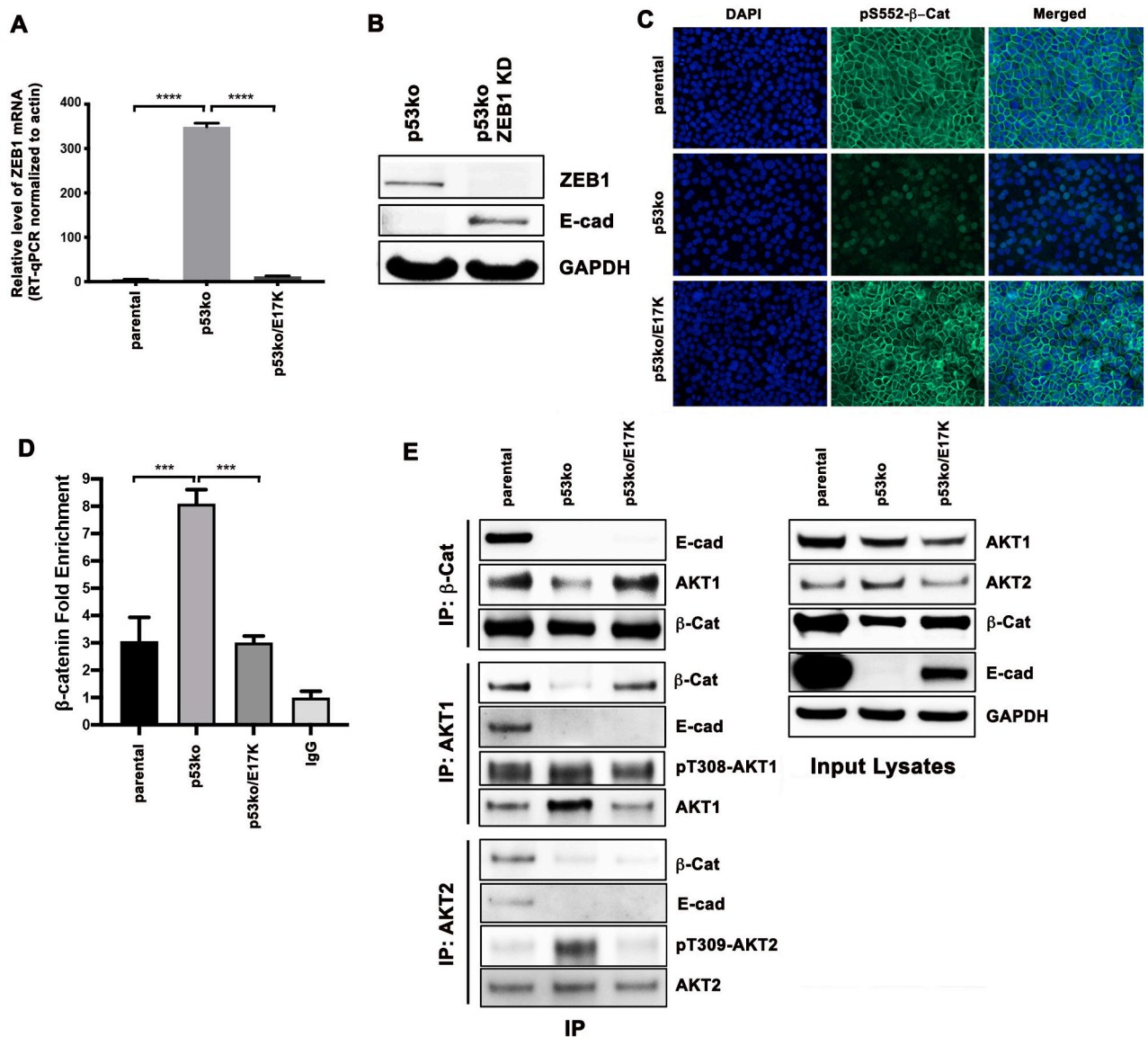


**Figure 3. Activated AKT1 results in increased membranous localization of β-catenin.**  
**A**, mRNA levels of *ZEB1* determined by RT-qPCR. **B**, Western blot of lysates from MCF-10A p53ko cells infected with a CRISPR/Cas9 lentivirus targeting *ZEB1*. **C**, Immunofluorescence of the MCF-10A isogenic cells using a β-catenin pSer552 specific antibody. **D**, β-catenin association with the *ZEB1* promoter at the chromatin level in the MCF-10A isogenic cells. Cells were subjected to chromatin immunoprecipitation (ChIP) using a β-catenin antibody. Relative fold of ChIP pull-down of the *ZEB1* promoter (β-catenin fold enrichment) was quantified by real-time qPCR, normalized by both input DNA and IgG values. Error bars represent mean ± SEM (n=3). *P* values were determined by 1-way ANOVA followed by Tukey post-hoc test. \*\*\**P*<0.001; \*\*\*\**P*<0.0001. **E**, Western blot of immunoprecipitates and input cell lysates from the MCF-10A isogenic cells with antibodies indicated.

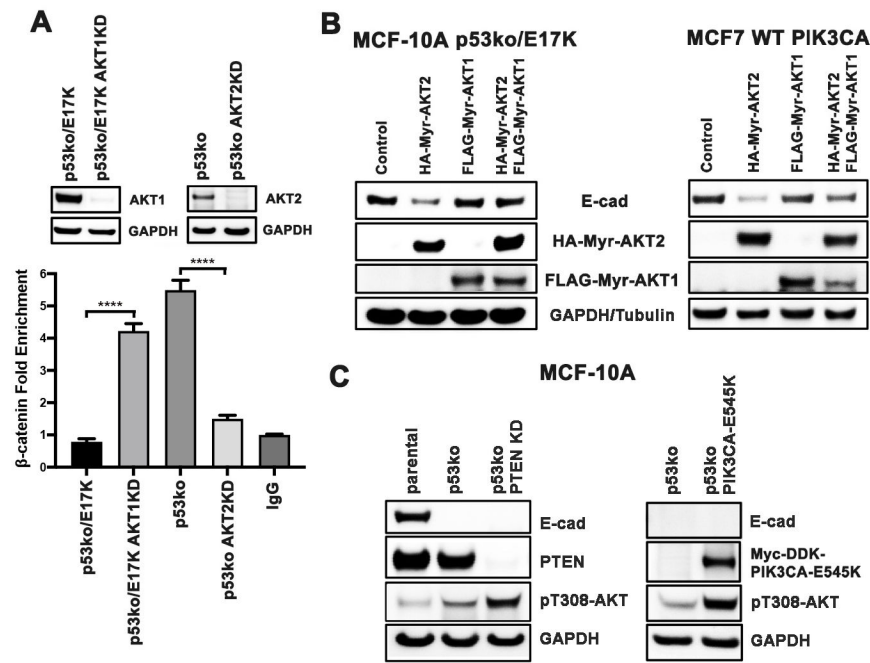


**Figure 4. AKT2, but not AKT1, increases the transcriptional activity of  $\beta$ -catenin on the *ZEB1* promoter, and decreases E-cadherin expression.**

**A**, p53ko/E17K cells were infected with a CRISPR/Cas9 lentivirus targeting *AKT1* and p53ko cells were infected with a CRISPR/Cas9 lentivirus targeting *AKT2*. Cells lysates were then subjected to ChIP using a  $\beta$ -catenin antibody. Top: Western blot of whole cell lysates from the indicated p53ko/E17K cells and p53ko cells before and after AKT1 knockdown (AKT1KD) or AKT2 knockdown (AKT2KD) as specified. Bottom: Relative fold of ChIP pull-down of the *ZEB1* promoter ( $\beta$ -catenin fold enrichment) was quantified by real-time qPCR, normalized by both input DNA and IgG values. Error bars represent mean  $\pm$  SEM (n=3). *P* values were determined by 1-way ANOVA followed by Tukey post-hoc test. \*\*\*\* *P*<0.0001. **B**, Western blots of lysates from MCF-10A p53ko/E17K or MCF-7 PIK3CA WT cells expressing HA tagged Myr-AKT2 and FLAG tagged Myr-AKT1 alone and in combination. **C**, Western blot of lysates from p53ko cells: Left: infected with PTEN CRISPR/Cas9 lentivirus; Right: infected with PIK3CA E545K lentivirus. Cell lysate of parental MCF-10A cells were used as an E-cadherin positive control.

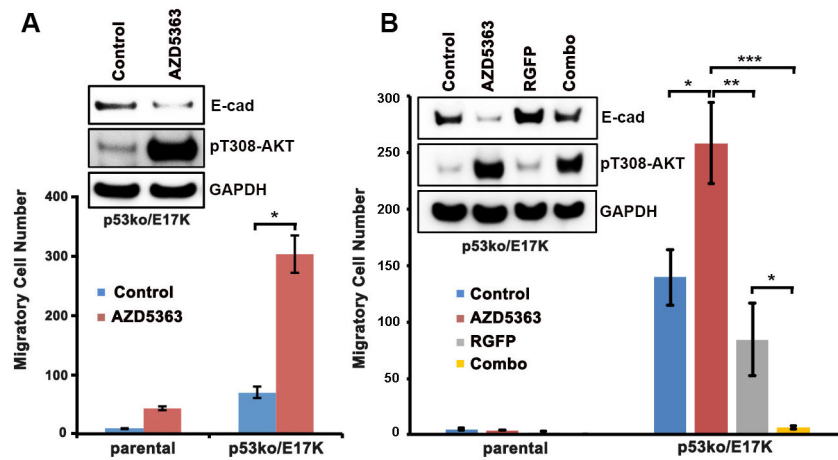


**Figure 5. The AKT kinase inhibitor AZD5363 enhanced the migration of parental and p53ko/E17K MCF-10A cells.**

**A**, Boyden chamber migration assays of parental and p53ko/E17K MCF-10A cells. Cells were treated with AZD5363 or DMSO control for 2 days. Top: Western blot of lysates from p53ko/E17K cells treated with DMSO control or AZD5363 (3  $\mu$ M). **B**, Top: Western blot of lysates from p53ko/E17K cells treated with DMSO control, AZD5363 (3  $\mu$ M), the HDAC inhibitor RGFP109 (5  $\mu$ M, RGFP) or both drugs (Combo). Bottom: Migration assay of MCF-10A cells treated with DMSO control, AZD5363, RGFP109 or a combination of both drugs. Error bars represent mean  $\pm$  SEM (n=2 to 5). *P* values were determined by Student's *t* test. \**P*<0.05; \*\**P*<0.01; \*\*\**P*<0.001. The results were repeated and confirmed.